calculate the singular integrals in this work. The approach can automatically cancel the singularity without using a variable change or coordinate transform and reduce the integrals to a one-fold numerical integration with a very simple integrand. Compared with the Duffy's method which requires a two-fold numerical integration, the approach could be more convenient in implementation and more efficient in calculation as illustrated by the numerical examples.

References

[1] W. C. Chew, M. S. Tong, and B. Hu, *Integral Equation Methods for Electromagnetic and Elastic Waves*. San Rafael, CA, USA: Morgan & Claypool, 2008.

[2] S. M. Rao, D. R. Wilton, and A. W. Glisson, "Electromagnetic scattering by surfaces of arbitrary shape," *IEEE Trans. Antennas Propag.*, vol. AP-30, no. 3, pp. 409–418, 1982.

[3] M. G. Duffy, "Quadrature over a pyramid or cube of integrands with a singularity at a vertex," *SIAM J. Numer. Anal.*, vol. 19, pp. 1260–1262, 1982.

[4] D. R. Wilton, S. M. Rao, A. W. Glisson, D. H. Schaubert, O. M. Al-Bundak, and C. M. Butler, "Potential integrals for uniform and linear source distributions on polygonal and polyhedral domains," *IEEE Trans. Antennas Propag.*, vol. 32, pp. 276–281, 1984.

[5] R. D. Graglia, "Static and dynamic potential integrals for linearly varying source distributions in two- and three-dimensional problems," *IEEE Trans. Antennas Propag.*, vol. 35, pp. 662–669, 1987.

[6] R. D. Graglia, "On the numerical integration of the linear shape functions times the 3-D Green's function or its Gradient on a plane triangle," *IEEE Trans. Antennas Propag.*, vol. 41, pp. 1448–1455, 1993.

[7] S. Caorsi, D. Moreno, and F. Sidoti, "Theoretical and numerical treatment of surface integrals involving the free-space Green's function," *IEEE Trans. Antennas Propag.*, vol. 41, no. 9, pp. 1296–1301, Sep. 1993.

[8] T. F. Eibert and V. Hansen, "On the calculation of potential integrals for linear source distributions on triangular domains," *IEEE Trans. Antennas Propag.*, vol. 43, pp. 1499–1502, Dec. 1995.

[9] P. Arcioni, M. Bressan, and L. Perregrini, "On the evaluation of the double surface integrals arising in the application of the boundary integral method to 3-D problems," *IEEE Trans. Microw. Theory Tech.*, vol. 45, pp. 436–439, Mar. 1997.

[10] M. J. Bluck, M. D. Pocock, and S. P. Walker, "An accurate method for the calculation of singular integrals arising in time-domain integral equation analysis of electromagnetic scattering," *IEEE Trans. Antennas Propag.*, vol. 45, no. 12, pp. 1793–1798, Dec. 1997.

[11] L. Rossi and P. J. Cullen, "On the fully numerical evaluation of the linear-shape function times the 3-D Green's function on a plane triangle," *IEEE Trans. Microw. Theory Tech.*, vol. 47, pp. 398–402, Apr. 1999.

[12] A. Herschlein, J. V. Hagen, and W. Wiesbeck, "Methods for the evaluation of regular, weakly singular and strongly singular surface reaction integrals arising in method of moments," *ACES J.*, vol. 17, no. 1, pp. 63–73, Mar. 2002.

[13] S. Järvenpää, M. Taskinen, and P. Ylä-Oijala, "Singularity extraction technique for integral equation methods with higher order basis functions on plane triangles and tetrahedra," *Int. J. Numer. Methods. Eng.*, vol. 58, pp. 1149–1165, 2003.

[14] D. J. Taylor, "Accurate and efficient numerical integration of weakly singular integrals in Galerkin EFIE solutions," *IEEE Trans. Antennas Propag.*, vol. 51, pp. 1630–1637, Jul. 2003.

[15] M. A. Khayat and D. R. Wilton, "Numerical evaluation of singular and near-singular potential integrals," *IEEE Trans. Antennas Propag.*, vol. 53, pp. 3180–3190, 2005.

[16] S. Järvenpää, M. Taskinen, and P. Ylä-Oijala, "Singularity subtraction technique for high-order polynomial vector basis functions on planar triangles," *IEEE Trans. Antennas Propag.*, vol. 54, no. 1, pp. 42–49, Jan. 2006.

[17] W.-H. Tang and S. D. Gedney, "An efficient evaluation of near singular surface integrals via the Khayat-Wilton transformation," *Microw. Opt. Tech. Lett.*, vol. 48, no. 8, pp. 1583–1586, 2006.

[18] M. S. Tong and W. C. Chew, "Super-hyper singularity treatment for solving 3D electric field integral equations," *Microw. Opt. Technol. Lett.*, vol. 49, pp. 1383–1388, 2007.

[19] P. W. Fink, D. R. Wilton, and M. A. Khayat, "Simple and efficient numerical evaluation of near-hypersingular integrals," *IEEE Antennas Wireless Propag. Lett.*, vol. 7, pp. 469–472, 2008.

[20] M. A. Khayat, D. R. Wilton, and P. W. Fink, "An improved transformation and optimized sampling scheme for the numerical evaluation of singular and near-singular potentials," *IEEE Antennas Wireless Propag. Lett.*, vol. 7, pp. 377–380, 2008.

[21] R. D. Graglia and G. Lombardi, "Machine precision evaluation of singular and nearly singular potential integrals by use of Gauss quadrature formulas for rational functions," *IEEE Trans. Antennas Propag.*, vol. 56, pp. 981–998, 2008.

[22] A. G. Polimeridis and T. V. Yioultsis, "On the direct evaluation of weakly singular integrals in Galerkin mixed potential integral equation formulations," *IEEE Trans. Antennas Propag.*, vol. 56, no. 9, pp. 3011–3019, Sep. 2008.

[23] G. T. Ruck, D. E. Barrick, W. D. Stuart, and C. K. Krichbaum, *Radar Cross Section Handbook*. New York, NY, USA: Plenum Press, 1970.

Electromagnetic Scattering by a Gyrotropic-Coated Conducting Sphere Illuminated From Arbitrary Spatial Angles

Yan Song, Chun-Ming Tse, and Cheng-Wei Qiu

***Abstract*—This communication presents the development of a Mie-based scattering theory for a gyrotropic-coated conducting sphere such that an arbitrary incident angle can be modeled analytically from an eigen-system determined by gyrotropic permittivity and permeability tensors. The incident and scattered fields can be expanded in terms of spherical vector wave functions (SVWFs). After the unknown scattering coefficients are obtained in the general gyrotropic media, the expansion coefficients associated with the eigenvectors and scattering coefficients can be determined by matching boundary conditions at the interfaces between different media. The scattering property of a gyrotropic object relies on where the illumination comes from, and hence it is different from the isotropic cases. This analytical approach enables the modeling of scattering by a gyrotropic-coated conducting sphere under arbitrary incident angles and polarizations.**

***Index Terms*—Azimuthal angle, electromagnetic scattering, gyrotropic media, gyrotropic ratio, radar cross section (RCS), radius ratio, spherical vector wave function.**

I. Introduction

Electromagnetic scattering of a conducting sphere coated with a gyrotropic media has been studied over the past few decades. The homogeneous sphere illuminated by a plane electromagnetic wave was developed by Lorenz and Mie, respectively [1] and [2], and it has been further extended in [3] and [4]. In the existing works, many numerical and analytical methods have been established and developed, for example, the finite difference time-domain (FDTD) [5], the integral equation method [6], Fourier transform [7], dyadic Green's functions [8], [9], artificial boundary transformation [10], and wave expansion [11].

Manuscript received July 17, 2011; revised October 31, 2012; accepted February 09, 2013. Date of publication March 19, 2013; date of current version May 29, 2013.

The authors are with Department of Electrical and Computer Engineering, National University of Singapore, Singapore 117576, Singapore (email: eleqc@nus.edu.sg).

Color versions of one or more of the figures in this communication are available online at http://ieeexplore.ieee.org.

Digital Object Identifier 10.1109/TAP.2013.2253294

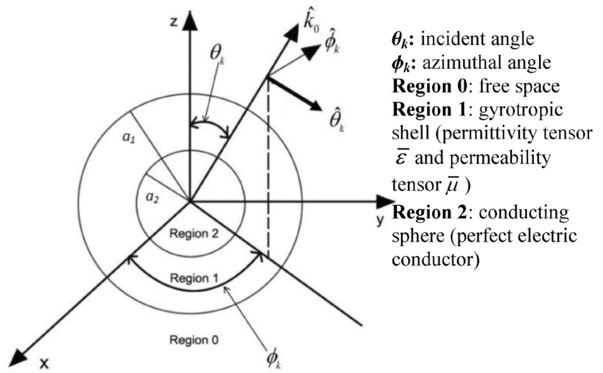

Fig. 1. The geometry of a conducting sphere coated with gyrotropic media.

However, most methods can only present the incoming wave's propagation along the z-axis. This problem is not important for isotropic objects because their radar cross section remains the same at the local observation frame no matter where the plane wave is incident upon it. Therefore, one can rotate the coordinate such that those reported methods could be applied to calculate the scattering and transform the results of the radar cross section (RCS) in the local frame back to the original laboratory frame. However, this problem becomes more critical for gyrotropic media as they have different behavior when the illumination angles change even at the local observation frame, making determination of the RCS difficult. Therefore, it motivates us to develop an analytical method to directly formulate the scattering property of gyrotropic objects in a fixed observation frame (which is always true), while the illumination comes from different angles. By exploiting the novel eigenwave expansion method developed for uniaxial spheres under arbitrary illumination angles (see, e.g., [12] and references therein), now the material in the core-shell system can be gyrotropic in both permittivity and permeability tensors and the illumination angle can be considered during SVWFs expansion. In this communication, the electromagnetic field is to be expanded in terms of the SVWFs in the gyrotropic medium. By applying the boundary conditions at the interface between the gyrotropic shell and PEC core, and another interface between the shell and free space, the unknown expansion coefficients associated with the eigenvector and scattering coefficients can be determined analytically. Not only did the numerical results demonstrate the validity of our proposed theory, but this communication shall also report some new results that the existing methods (not only analytical but also numerical) are not able to deal with.

II. Formulation

In Fig. 1, it shows that a conducting sphere is coated with a gyrotropic medium. The coated sphere with an outer radius a_1 and an inner radius a_2 is located at the coordinate origin. Hence the core-shell system is divided into three distinct regions, namely, region 0 for the free space, region 1 for the gyrotropic shell (characterized by the permittivity and permeability tensors), and region 2 for the conducting sphere (perfect electric conductor). The incident wave impinged on the coated object comes from an arbitrary incident angle ($\boldsymbol{\theta_k}$) and azimuthal angle ($\boldsymbol{\phi_k}$). The time dependence of $\exp(-i\omega t)$ is assumed but suppressed throughout.

The permittivity and permeability tensors of the gyrotropic media can be characterized by

$$\bar{\varepsilon} = \varepsilon_s \begin{bmatrix} \varepsilon_r & -i\varepsilon_g & 0 \\ i\varepsilon_g & \varepsilon_r & 0 \\ 0 & 0 & 1 \end{bmatrix}; \quad \bar{\mu} = \mu_s \begin{bmatrix} \mu_r & -i\mu_g & 0 \\ i\mu_g & \mu_r & 0 \\ 0 & 0 & 1 \end{bmatrix} \tag{1}$$

The constitutive relations inside the gyrotropic medium are expressed as

$$\mathbf{D}_{\rm int} = \bar{\varepsilon} \cdot \mathbf{E}_{\rm int}, \quad \mathbf{B}_{\rm int} = \bar{\mu} \cdot \mathbf{H}_{\rm int} \tag{2}$$

Substituting (2) into the source-free Maxwell equations, the wave equation is obtained as follows,

$$\nabla \times \nabla \times \left[\varepsilon_s \bar{\varepsilon}^{-1} \cdot (\nabla \times \mu_s \bar{\mu}^{-1} \cdot \mathbf{B}_{\rm int})\right] - k_s^2 \mathbf{B}_{\rm int} = 0 \tag{3}$$

$$\varepsilon_s \bar{\varepsilon}^{-1} = \begin{bmatrix} \varepsilon'_r & -i\varepsilon'_g & 0 \\ i\varepsilon'_g & \varepsilon'_r & 0 \\ 0 & 0 & 1 \end{bmatrix}; \quad \mu_s \bar{\mu}^{-1} = \begin{bmatrix} \mu'_r & -i\mu'_g & 0 \\ i\mu'_g & \mu'_r & 0 \\ 0 & 0 & 1 \end{bmatrix} \tag{4}$$

where $k_s^2 = \omega^2 \varepsilon_s \mu_s$, and ε'_r, ε'_g, μ'_r and μ'_g are shown in the Appendix. $\mathbf{B}_{\rm int}$ in region 1 can be expanded in terms of the SVWFs.

$$\mathbf{B_{int}} = \sum_{n,m} \bar{E}_{mn} \Big[d_{mn} \mathbf{M}_{mn}^{(1)}(k, \mathbf{r}) + c_{mn} \mathbf{N}_{mn}^{(1)}(k, \mathbf{r}) + u_{mn} \mathbf{M}_{mn}^{(3)}(k, \mathbf{r}) + v_{mn} \mathbf{N}_{mn}^{(3)}(k, \mathbf{r}) \Big] \tag{5}$$

where n runs from 1 to ∞, and m runs from $-n$ to n. In practice, the expansion is uniformly convergent and can be truncated at $n = n_c = x + 4x^{1/3} + 2$ [13], where x denotes the size parameter $x = k_0 a_1$. Employing the relations between SVWFs, the following sets of equations can be obtained

$$\mu_s \bar{\mu}^{-1} \cdot \mathbf{M}_{uv} = \sum_{q=0}^{+\infty} \sum_{p=-q}^{+q} \left[\tilde{g}_{pq}^{uv} \mathbf{M}_{pq} + \tilde{e}_{pq}^{uv} \mathbf{N}_{pq} + \tilde{f}_{pq}^{uv} \mathbf{L}_{pq} \right] \tag{6.1}$$

$$\mu_s \bar{\mu}^{-1} \cdot \mathbf{N}_{uv} = \sum_{q=0}^{+\infty} \sum_{p=-q}^{+q} \left[\bar{g}_{pq}^{uv} \mathbf{M}_{pq} + \bar{e}_{pq}^{uv} \mathbf{N}_{pq} + \bar{f}_{pq}^{uv} \mathbf{L}_{pq} \right] \tag{6.2}$$

$$\varepsilon_s \bar{\varepsilon}^{-1} \cdot \mathbf{M}_{mn} = \sum_{q=0}^{+\infty} \sum_{p=-q}^{+q} \left[\tilde{o}_{pq}^{mn} \mathbf{M}_{pq} + \tilde{p}_{pq}^{mn} \mathbf{N}_{pq} + \tilde{q}_{pq}^{mn} \mathbf{L}_{pq} \right] \tag{6.3}$$

$$\varepsilon_s \bar{\varepsilon}^{-1} \cdot \mathbf{N}_{mn} = \sum_{q=0}^{+\infty} \sum_{p=-q}^{+q} \left[\bar{o}_{pq}^{mn} \mathbf{M}_{pq} + \bar{p}_{pq}^{mn} \mathbf{N}_{pq} + \bar{q}_{pq}^{mn} \mathbf{L}_{pq} \right] \tag{6.4}$$

where the unknown expansion coefficients

$$\bar{g}_{pq}^{uv}, \bar{e}_{pq}^{uv}, \bar{f}_{pq}^{uv}, \tilde{g}_{pq}^{uv}, \tilde{e}_{pq}^{uv}, \tilde{f}_{pq}^{uv}, \bar{o}_{pq}^{mn}, \bar{p}_{pq}^{mn}, \bar{q}_{pq}^{mn}, \tilde{o}_{pq}^{mn}, \tilde{p}_{pq}^{mn} \text{ and } \tilde{q}_{pq}^{mn}$$

are given in the Appendix. Substituting (6) into (5),

$$\begin{aligned} \mu_s \bar{\mu}^{-1} \cdot \mathbf{B}_{\rm int} &= \sum_{n=1}^{+\infty} \sum_{m=-n}^{+n} \bar{E}_{pq} \Big(\bar{d}_{pq} \mathbf{M}_{pq}^{(1)} + \bar{c}_{pq} \mathbf{N}_{pq}^{(1)} \\ &\quad + \bar{w}_{pq} \mathbf{L}_{pq}^{(1)} + \bar{u}_{pq} \mathbf{M}_{pq}^{(3)} \\ &\quad + \bar{v}_{pq} \mathbf{N}_{pq}^{(3)} + \bar{y}_{pq} \mathbf{L}_{pq}^{(3)} \Big) \\ &\quad + \bar{w}_{00} \mathbf{L}_{00}^{(1)} + \bar{y}_{00} \mathbf{L}_{00}^{(3)} \end{aligned} \tag{7.1}$$

$$\begin{aligned} \varepsilon_s \bar{\varepsilon}^{-1} \cdot (\nabla \times \mu_s \bar{\mu}^{-1} \cdot \mathbf{B}_{\rm int}) &= k \sum_{n.m} \bar{E}_{mn} \Big(\bar{\bar{c}}_{mn} \mathbf{M}_{mn}^{(1)} + \bar{\bar{d}}_{mn} \mathbf{N}_{mn}^{(1)} + \bar{\bar{w}}_{mn} \mathbf{L}_{pq}^{(1)} \\ &\quad + \bar{\bar{v}}_{mn} \mathbf{M}_{pq}^{(3)} + \bar{\bar{u}}_{mn} \mathbf{N}_{mn}^{(3)} + \bar{\bar{y}}_{mn} \mathbf{L}_{mn}^{(3)} \Big) \\ &\quad + \bar{\bar{w}}_{00} \mathbf{L}_{00}^{(1)} + \bar{\bar{y}}_{00} \mathbf{L}_{00}^{(3)} \end{aligned} \tag{7.2}$$

The coefficients $\bar{c}_{pq}, \bar{d}_{pq}, \bar{w}_{pq}, \bar{v}_{pq}, \bar{u}_{pq}, \bar{y}_{pq}, \bar{w}_{00}$ and $\bar{y}_{00}$ can be found in the Appendix. In (7), $\bar{E}_{mn} = i^n E_0 C_{mn}$ where E_0 is the amplitude of the incident electric field and C_{mn} is given in the Appendix. Note that SVWFs satisfy the relations

$$\nabla \times \mathbf{M}_{mn} = k\mathbf{N}_{mn}; \quad \nabla \times \mathbf{N}_{mn} = k\mathbf{M}_{mn}; \quad \nabla \times \mathbf{L}_{mn} = 0 \tag{8}$$

Hence the following equations can be obtained by substituting (7) and (5) into (3)

$$\begin{aligned}\nabla \times \Bigg[k \sum_{m,n} \bar{E}_{mn} \Big(&\bar{\bar{c}}_{mn}\mathbf{M}_{mn}^{(1)} + \bar{\bar{d}}_{mn}\mathbf{N}_{mn}^{(1)} + \bar{\bar{w}}_{mn}\mathbf{L}_{mn}^{(1)} \\ &+\bar{\bar{v}}_{mn}\mathbf{M}_{mn}^{(3)} + \bar{\bar{u}}_{mn}\mathbf{N}_{mn}^{(3)} + \bar{\bar{y}}_{mn}\mathbf{L}_{mn}^{(3)} \Big) \\ &+\bar{\bar{w}}_{00}\mathbf{L}_{mn}^{(1)} + \bar{\bar{y}}_{00}\mathbf{L}_{mn}^{(3)} \Bigg] \\ - k_s^2 \Bigg[\sum_{m,n} \bar{E}_{mn} \Big(&c_{mn}\mathbf{N}_{mn}^{(1)} \\ &+d_{mn}\mathbf{M}_{mn}^{(1)} + v_{mn}\mathbf{N}_{mn}^{(3)} + u_{mn}\mathbf{M}_{mn}^{(3)} \Big) \Bigg] = 0\end{aligned} \tag{9}$$

$$\bar{\bar{d}}_{mn} = \sum_{q,p} \frac{\bar{E}_{pq}}{\bar{E}_{mn}} \left(\bar{p}_{mn}^{pq}\bar{d}_{pq} + \tilde{p}_{mn}^{pq}\bar{c}_{pq} \right) \tag{10.1}$$

$$\bar{\bar{c}}_{mn} = \sum_{q,p} \frac{\bar{E}_{pq}}{\bar{E}_{mn}} \left(\bar{o}_{mn}^{pq}\bar{d}_{pq} + \tilde{o}_{mn}^{pq}\bar{c}_{pq} \right) \tag{10.2}$$

$$\bar{\bar{w}}_{mn} = \sum_{q,p} \frac{\bar{E}_{pq}}{\bar{E}_{mn}} \left(\bar{q}_{mn}^{pq}\bar{d}_{pq} + \tilde{q}_{mn}^{pq}\bar{c}_{pq} \right) \tag{10.3}$$

$$\begin{aligned}\bar{\bar{w}}_{00} &= k \sum_{q,p} \bar{E}_{pq} \left(\bar{q}_{00}^{pq}\bar{d}_{pq} + \tilde{q}_{00}^{pq}\bar{c}_{pq} \right) \\ &= k \left[\bar{E}_{02}\bar{q}_{00}^{02}\bar{d}_{02} + \bar{E}_{01}\tilde{q}_{00}^{01}\bar{c}_{01} \right]\end{aligned} \tag{10.4}$$

$$\bar{\bar{u}}_{mn} = \sum_{q,p} \frac{\bar{E}_{pq}}{\bar{E}_{mn}} \left(\bar{p}_{mn}^{pq}\bar{u}_{pq} + \tilde{p}_{mn}^{pq}\bar{v}_{pq} \right) \tag{10.5}$$

$$\bar{\bar{v}}_{mn} = \sum_{q,p} \frac{\bar{E}_{pq}}{\bar{E}_{mn}} \left(\bar{o}_{mn}^{pq}\bar{u}_{pq} + \tilde{o}_{mn}^{pq}\bar{v}_{pq} \right) \tag{10.6}$$

$$\bar{\bar{y}}_{mn} = \sum_{q,p} \frac{\bar{E}_{pq}}{\bar{E}_{mn}} \left(\bar{q}_{mn}^{pq}\bar{u}_{pq} + \tilde{q}_{mn}^{pq}\bar{v}_{pq} \right) \tag{10.7}$$

$$\begin{aligned}\bar{\bar{y}}_{00} &= k \sum_{q,p} \bar{E}_{pq} \left(\bar{q}_{00}^{pq}\bar{u}_{pq} + \tilde{q}_{00}^{pq}\bar{v}_{pq} \right) \\ &= k \left[\bar{E}_{02}\bar{q}_{00}^{02}\bar{u}_{02} + \bar{E}_{01}\tilde{q}_{00}^{01}\bar{v}_{01} \right]\end{aligned} \tag{10.8}$$

After lengthy mathematical manipulation for (9), the following eigen-system is given, where $\lambda = k_s^2/k^2$,

$$\begin{pmatrix} \tilde{P} & \bar{P} & \tilde{P} & \bar{P} \\ \tilde{O} & \bar{O} & \tilde{O} & \bar{O} \end{pmatrix} \begin{pmatrix} d \\ c \\ u \\ v \end{pmatrix} = \lambda \begin{pmatrix} d \\ c \\ u \\ v \end{pmatrix} \tag{11}$$

$$\tilde{P}_{mn,uv} = \sum_{q,p} \frac{\bar{E}_{uv}}{\bar{E}_{mn}} \left(\bar{p}_{mn}^{pq}\tilde{g}_{pq}^{uv} + \tilde{p}_{mn}^{pq}\tilde{e}_{pq}^{uv} \right) \tag{12.1}$$

$$\bar{P}_{mn,uv} = \sum_{q,p} \frac{\bar{E}_{uv}}{\bar{E}_{mn}} \left(\bar{p}_{mn}^{pq}\bar{g}_{pq}^{uv} + \tilde{p}_{mn}^{pq}\bar{e}_{pq}^{uv} \right) \tag{12.2}$$

$$\tilde{O}_{mn,uv} = \sum_{q,p} \frac{\bar{E}_{uv}}{\bar{E}_{mn}} \left(\bar{o}_{mn}^{pq}\tilde{g}_{pq}^{uv} + \tilde{o}_{mn}^{pq}\tilde{e}_{pq}^{uv} \right) \tag{12.3}$$

$$\bar{O}_{mn,uv} = \sum_{q,p} \frac{\bar{E}_{uv}}{\bar{E}_{mn}} \left(\bar{o}_{mn}^{pq}\bar{g}_{pq}^{uv} + \tilde{o}_{mn}^{pq}\bar{e}_{pq}^{uv} \right) \tag{12.4}$$

The subscripts mn and superscripts uv denote the row and column indices, respectively. Equation (11) is an eigen-system of eigenvalue $\lambda_{l.}$ and the eigenvectors $(d_{mn,l}, c_{mn,l})^T$ where l denotes the index of eigenvalues and corresponding eigenvectors. A new function $\mathbf{V}_l$ is constructed based on the eigenvectors, where $k_l = k_s/\sqrt{\lambda_l}$:

$$\begin{aligned}\mathbf{V}_l = -\frac{k_l}{\omega} \sum_{n,m} \bar{E}_{mn} \Big[&d_{mn,l}\mathbf{M}_{mn}^{(1)}(k_l, \mathbf{r}) + c_{mn,l}\mathbf{N}_{mn}^{(1)}(k_l, \mathbf{r}) \\ &+ u_{mn,l}\mathbf{M}_{mn}^{(3)}(k_l, \mathbf{r}) + v_{mn,l}\mathbf{N}_{mn}^{(3)}(k_l, \mathbf{r}) \Big]\end{aligned} \tag{13}$$

Since $\nabla \cdot \mathbf{V}_l = 0$, (3) and (5) can be rewritten as

$$\nabla \times \left[\varepsilon_s \bar{\varepsilon}^{-1} \cdot \nabla \times (\mu_s \bar{\mu}^{-1} \cdot \mathbf{V}_l) \right] - k_s^2 \mathbf{V}_l = 0 \tag{14}$$

$$\begin{aligned}\mathbf{B}_{\text{int}} &= \sum_{l=1}^{2n_c(n_c+2)} \alpha_l \mathbf{V}_l \\ &= -\sum_l \alpha_l \frac{k_l}{\omega} \sum_{n,m} \bar{E}_{mn} \Big[d_{mn,l}\mathbf{M}_{mn}^{(1)}(k_l, \mathbf{r}) \\ &\quad + c_{mn,l}\mathbf{N}_{mn}^{(1)}(k_l, \mathbf{r}) \\ &\quad + u_{mn,l}\mathbf{M}_{mn}^{(3)}(k_l, \mathbf{r}) + v_{mn,l}\mathbf{N}_{mn}^{(3)}(k_l, \mathbf{r}) \Big]\end{aligned} \tag{15}$$

The expansion coefficients α_l can be determined by matching the boundary condition between the sphere and free space. $\mathbf{H}_{\text{int}}$ can thus be expressed based on (2) and (15). Then $\mathbf{E}_{\text{int}}$ can be formulated from the Maxwell's equation.

$$\begin{aligned}\mathbf{H}_{\text{int}} &= \bar{\mu}^{-1} \cdot \mathbf{B}_{\text{int}} \\ &= -\sum_{m,n} \bar{E}_{mn} \sum_l \alpha_l \frac{k_l}{\mu_s \omega} \Big[\bar{d}_{mn,l}\mathbf{M}_{mn}^{(1)}(k_l, \mathbf{r}) \\ &\quad + \bar{c}_{mn,l}\mathbf{N}_{mn}^{(1)}(k_l, \mathbf{r}) + \bar{w}_{mn,l}\mathbf{L}_{mn}^{(1)}(k_l, \mathbf{r}) \\ &\quad + \bar{u}_{mn,l}\mathbf{M}_{mn}^{(3)}(k_l, \mathbf{r}) + \bar{v}_{mn,l}\mathbf{N}_{mn}^{(3)}(k_l, \mathbf{r}) \Big]\end{aligned} \tag{16}$$

$$\begin{aligned}\mathbf{E}_{\text{int}} &= \frac{i}{\omega} \bar{\varepsilon}^{-1} \cdot (\nabla \times \mathbf{H}_{\text{int}}) \\ &= -i \sum_{n,m} \bar{E}_{mn} \sum_l \alpha_l \Big[c_{mn,l}\mathbf{M}_{mn}^{(1)}(k_l, \mathbf{r}) \\ &\quad + d_{mn,l}\mathbf{N}_{mn}^{(1)}(k_l, \mathbf{r}) + \frac{\bar{\bar{w}}_{mn,l}}{\lambda}\mathbf{L}_{mn}^{(1)}(k_l, \mathbf{r}) \\ &\quad + v_{mn,l}\mathbf{M}_{mn}^{(3)}(k_l, \mathbf{r}) + u_{mn,l}\mathbf{N}_{mn}^{(3)}(k_l, \mathbf{r}) \\ &\quad + \frac{\bar{\bar{y}}_{mn,l}}{\lambda}\mathbf{L}_{mn}^{(3)}(k_l, \mathbf{r}) \Big] \\ &\quad - i \sum_l \alpha_l \left[\frac{\bar{\bar{w}}_{00,l}}{\lambda}\mathbf{L}_{00}^{(1)}(k_l, \mathbf{r}) + \frac{\bar{\bar{y}}_{00,l}}{\lambda}\mathbf{L}_{00}^{(3)}(k_l, \mathbf{r}) \right]\end{aligned} \tag{17}$$

To solve those expansion coefficients, the incident fields are to be expanded in terms of SVWFs which will make matching the boundary condition easier

$$\mathbf{E}_i = -\sum_{n,m} i\bar{E}_{mn} \left[p_{mn}\mathbf{N}_{mn}^{(1)}(k_0, \mathbf{r}) + q_{mn}\mathbf{M}_{mn}^{(1)}(k_0, \mathbf{r}) \right] \tag{18}$$

$$\mathbf{H}_i = -\frac{k_0}{\mu_0 \omega} \sum_{n,m} \bar{E}_{mn} \left[q_{mn}\mathbf{N}_{mn}^{(1)}(k_0, \mathbf{r}) + p_{mn}\mathbf{M}_{mn}^{(1)}(k_0, \mathbf{r}) \right] \tag{19}$$

The coefficients p_{mn} and q_{mn} associated with the incident wave are given in the Appendix. The scattered fields can be represented in a similar fashion

$$\mathbf{E}_s = \sum_{n,m} i\bar{E}_{mn} \left[a_{mn}\mathbf{N}_{mn}^{(3)}(k_0, \mathbf{r}) + b_{mn}\mathbf{M}_{mn}^{(3)}(k_0, \mathbf{r}) \right] \tag{20}$$

$$\mathbf{H}_s = \frac{k_0}{\mu_0 \omega} \sum_{n,m} \bar{E}_{mn} \left[b_{mn}\mathbf{N}_{mn}^{(3)}(k_0, \mathbf{r}) + a_{mn}\mathbf{M}_{mn}^{(3)}(k_0, \mathbf{r}) \right] \tag{21}$$

where $k_0^2 = \omega^2 \epsilon_0 \mu_0$. Applying boundary conditions at the surface of the conducting sphere (size parameters $x_0 = k_0 a_2$), the following equations are obtained:

$$v_{mn,l} = -\frac{\psi_n(k_l a_2)}{\xi_n(k_l a_2)} c_{mn,l} = -\frac{1}{S_n(k_l a_2)} c_{mn,l} \tag{22.1}$$

$$u_{mn,l} = -\frac{\psi_n'(k_l a_2)}{\xi_n'(k_l a_2)} d_{mn,l} = -\frac{1}{S_n'(k_l a_2)} d_{mn,l} \tag{22.2}$$

$$\bar{y}_{mn,l} = -\frac{\psi_n(k_l a_2)}{\xi_n(k_l a_2)} \bar{w}_{mn,l} = -\frac{1}{S_n(k_l a_2)} \bar{w}_{mn,l} \tag{22.3}$$

Similarly, matching boundary conditions at the interface between the free space and the gyrotropic shell (size parameter $x = k_0 a_1$), the following equations are obtained, where $m_s = k_s/k_0; \bar{k}_l = k_l/k_s; \psi_n(z) = z j_n(z)$ and $\xi_n(z) = z h_n^{(1)}(z)$ are the Riccati-Bessel functions, $j_n(kr)$ and $h_n^{(1)}(kr)$ are the spherical Bessel functions of the first kind and third kind, respectively.

$$\begin{aligned}
&\left[\frac{\xi_n'(x)}{\psi_n'(x)}\right] a_{mn} + \sum_l \left[\frac{1}{m_s \bar{k}_l} \frac{\psi_n'(\bar{k}_l m_s x)}{\psi_n'(x)} d_{mn,l}\right.\\
&\quad \left. + \frac{1}{m_s \bar{k}_l} \frac{\xi_n'(\bar{k}_l m_s x)}{\psi_n'(x)} u_{mn,l}\right] \alpha_l\\
&\quad + \sum_l \left[\frac{1}{m_s \bar{k}_l \lambda_l} \frac{j_n(\bar{k}_l m_s x)}{\psi_n'(x)} \bar{w}_{mn,l}\right.\\
&\quad \left. + \frac{1}{m_s \bar{k}_l \lambda_l} \frac{h_n^{(1)}(\bar{k}_l m_s x)}{\psi_n'(x)} \bar{\bar{y}}_{mn,l}\right] \alpha_l = p_{mn}
\end{aligned} \tag{23.1}$$

$$\begin{aligned}
&\left[\frac{\xi_n(x)}{\psi_n(x)}\right] b_{mn} + \sum_l \left[\frac{1}{m_s \bar{k}_l} \frac{\psi_n(\bar{k}_l m_s x)}{\psi_n(x)} c_{mn,l}\right.\\
&\quad \left. + \frac{1}{m_s \bar{k}_l} \frac{\xi_n(\bar{k}_l m_s x)}{\psi_n(x)} v_{mn,l}\right] \alpha_l = q_{mn}
\end{aligned} \tag{23.2}$$

$$\begin{aligned}
&\left[\frac{\xi_n(x)}{\psi_n(x)}\right] a_{mn} + \sum_l \left[\frac{\mu_0}{\mu_s} \frac{\psi_n(\bar{k}_l m_s x)}{\psi_n(x)} \bar{d}_{mn,l}\right.\\
&\quad \left. + \frac{\mu_0}{\mu_s} \frac{\xi_n(\bar{k}_l m_s x)}{\psi_n(x)} \bar{u}_{mn,l}\right] \alpha_l = p_{mn}
\end{aligned} \tag{23.3}$$

$$\begin{aligned}
&\left[\frac{\xi_n'(x)}{\psi_n'(x)}\right] b_{mn} + \sum_l \left[\frac{\mu_0}{\mu_s} \frac{\psi_n'(\bar{k}_l m_s x)}{\psi_n'(x)} \bar{c}_{mn,l}\right.\\
&\quad \left. + \frac{\mu_0}{\mu_s} \frac{\xi_n'(\bar{k}_l m_s x)}{\psi_n'(x)} \bar{v}_{mn,l}\right] \alpha_l + \sum_l \left[\frac{\mu_0}{\mu_s} \frac{j_n(\bar{k}_l m_s x)}{\psi_n'(x)} \bar{w}_{mn,l}\right.\\
&\quad \left. + \frac{\mu_0}{\mu_s} \frac{h_n^{(1)}(\bar{k}_l m_s x)}{\psi_n'(x)} \bar{y}_{mn,l}\right] \alpha_l = q_{mn}
\end{aligned} \tag{23.4}$$

Equation (23) can be formulated in the following form

$$\begin{aligned}
&\bar{\Lambda}_{mn,uv} a_{mn} + \bar{U}_{mn,l} \tilde{\alpha}_l = p_{mn};\\
&\Lambda_{mn,uv} b_{mn} + V_{mn,l} \tilde{\alpha}_l = p_{mn}\\
&\Lambda_{mn,uv} a_{mn} + U_{mn,l} \tilde{\alpha}_l = q_{mn};\\
&\bar{\Lambda}_{mn,uv} b_{mn} + \bar{V}_{mn,l} \tilde{\alpha}_l = q_{mn}
\end{aligned} \tag{24}$$

Equation (24) can be represented in a matrix form

$$\begin{aligned}
&\begin{pmatrix} \bar{\Lambda} & 0 \\ 0 & \Lambda \end{pmatrix} \begin{pmatrix} a \\ b \end{pmatrix} + \begin{pmatrix} \bar{U} \\ U \end{pmatrix} \tilde{\alpha}_l = \begin{pmatrix} p \\ q \end{pmatrix}\\
&\begin{pmatrix} \Lambda & 0 \\ 0 & \bar{\Lambda} \end{pmatrix} \begin{pmatrix} a \\ b \end{pmatrix} + \begin{pmatrix} \bar{V} \\ V \end{pmatrix} \tilde{\alpha}_l = \begin{pmatrix} p \\ q \end{pmatrix}.
\end{aligned} \tag{25}$$

Thus, the unknown coefficients of electromagnetic fields in the gyrotropic spherical medium can be obtained, and the unknown coefficients a_{mn} and b_{mn} of scattered fields in free space can be calculated using the aforementioned method. With the scattering coefficients obtained from (20) and (21), RCS for different incident angles can be obtained using formulas presented in the Appendix.

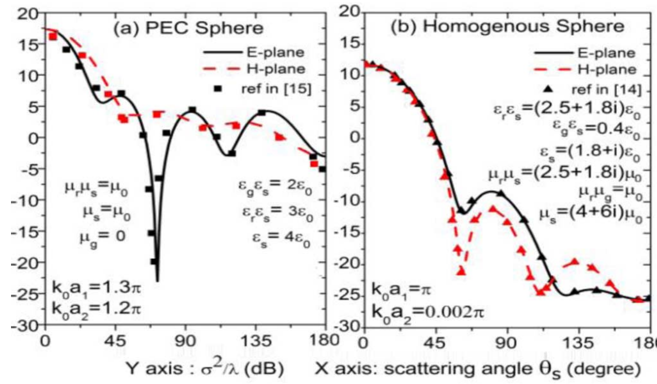

Fig. 2. (a) RCS versus the scattering angle of a non-magnetic sphere (b) RCS versus the scattering angle in a homogeneous gyrotropic sphere.

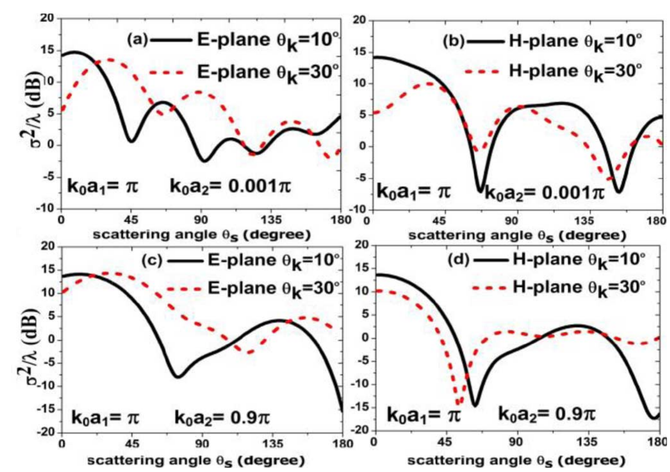

Fig. 3. RCS versus scattering angle in E-plane and H-plane under $\theta_k = 10°$ and 30° for two radius ratios. $\varepsilon_r\varepsilon_s = 2\varepsilon_0, \varepsilon_g\varepsilon_s = 0.4\varepsilon_0, \varepsilon_s = 4\varepsilon_0, \mu_r\mu_s = 2\mu_0, \mu_s = 4\mu_0$ and $\mu_g\mu_s = 0.4\,\mu_0$.

III. Numerical Results and Discussion

Our proposed approach is validated numerically by comparing with the results obtained from other existing approaches. Nevertheless, it is clear that the existing approaches can only be comparable to our approach in the case of a plane wave incident along the z-axis. Fig. 2 illustrates the agreement between our obtained bistatic RCS and those obtained by the Fourier transform method [14] and the multilevel boundary-element integration method [15], in both situations of a bare homogenous gyrotropic sphere and a gyrotropic-coated conducting sphere.

In Fig. 3(a) and (b), the inner radius is assumed to be extremely small $(k_0 a_2 = 0.001\pi)$, leading to a homogeneous gyrotropic sphere with $k_0 a_1 = \pi$. It is clear that the far-field RCS differs drastically when the illumination angle θ_k changes. Only the forward scattering is insensitive to the variation of θ_k. The RCS at the observation angle $\theta_s = 67°$ in the H-plane increases significantly as the incident angle increases from 10° to 30°. It implies that we can manipulate the scattering intensity at a particular observation angle by launching the same incidence along a particular direction. It can thus be concluded that RCS patterns of a general gyrotropic-coated PEC sphere $(k_0 a_2 = 0.9\pi)$ will be affected by the illumination angle, as Fig. 3(c) and (d) show.

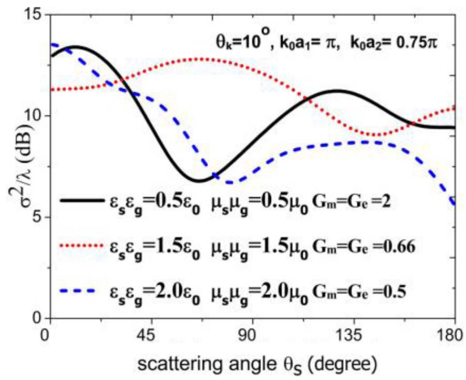

Fig. 4. RCS versus scattering angle θ_s in E-plane, $\varepsilon_s\varepsilon_r = \varepsilon_0, \varepsilon_s = 2.5\varepsilon_0$ and $\mu_s\mu_r = \mu_0, \mu_s = 2.5\ \mu_0$.

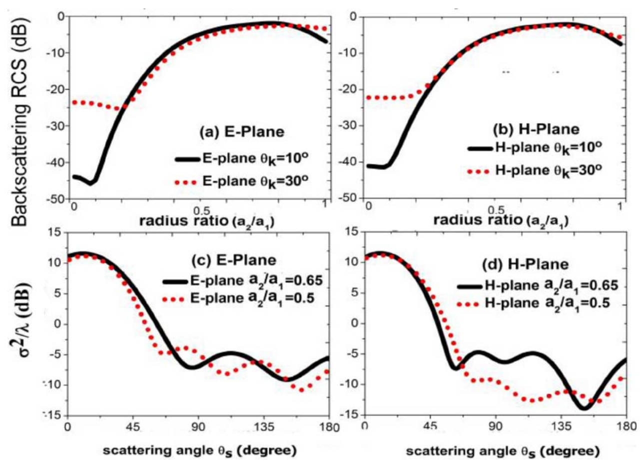

Fig. 5. Backscattering RCS versus radius ratio (0 to 1) in (a) E-plane (b) H-plane under $\theta_k = 10^\circ$ and 30°. $k_0a_1 = 0.5\pi, \varepsilon_r\varepsilon_s = \varepsilon_0, \varepsilon_g\varepsilon_s = 0.4\varepsilon_0, \varepsilon_s = 2\varepsilon_0, \mu_r\mu_s = \mu_0, \mu_s = 2\ \mu_0$ and $\mu_g\mu_s = 0.4\ \mu_0$. RCS versus scattering angle in (c) E-plane (d) H-plane at two fixed radius ratios of 0.65 and 0.5, for lossy coatings. $\varepsilon_r\varepsilon_s = (2+0.2i)\varepsilon_0, \varepsilon_g\varepsilon_s = 0.4\varepsilon_0, \varepsilon_s = (4+0.4i)\varepsilon_0$, $\mu_r\mu_s = (2+0.2i)\varepsilon\mu_0, \mu_g\mu_s = 0.4\ \mu_0, \mu_s = (4+0.4i)\mu_0, k_0a_1 = \pi$ and $\theta_k = 10^\circ$.

In order to quantify the effects of the material's gyrotropy on the scattering, we define electric-gyrotropic contrast ($G_e = \varepsilon_r/\varepsilon_g$) and magnetic-gyrotropic contrast ($G_m = \mu_r/\mu_g$), respectively. Fig. 4 shows that the gyrotropic contrast plays an important role in controlling RCS in a fixed observation frame. For example, when $G_m = G_e > 1$ (the off-diagonal parameter is smaller than the diagonal parameter), RCS can reach its minimum near $\theta_s = 60^\circ$. On the contrary, when $G_m = G_e < 1$ (off-diagonal parameters become more dominant), RCS has sensitive dependence of gyrotropic contrast, e.g., when the gyrotropic contrast decreases from 0.66 to 0.5, RCS has been decreased over wide observation angles except for in the forward direction.

Larger backscattering in the E-plane and the H-plane will be observed in Fig. 5(a) and (b), if the radius ratio is smaller than 0.3 as the incident angle increases to 30°. Fig. 5(c) and (d) demonstrates the effect of the radius ratio on conducting spheres coated with lossy gyrotropic media. It can be seen that the RCS decreases in both E- and H-planes at $\theta_s = 30^\circ$ as the radius ratio increases. Since we stress that the illumination angles are crucial for the scattering of a gyrotropic object, Fig. 6 shows us how the backscattering is influenced by the incident and azimuthal angles.

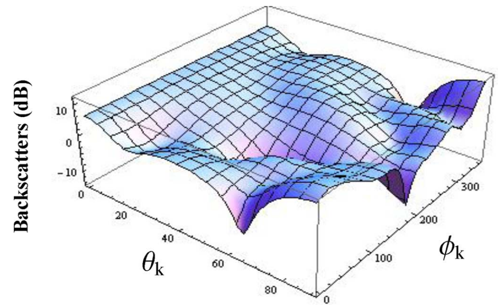

Fig. 6. Backscattering versus incident angle θ_k (0° to 90°) and azimuthal angle ϕ_k (0° to 360°), size parameter $k_0a_1 = \pi$ and $k_0a_2 = 0.5\pi$, $\epsilon_s = 4\varepsilon_0$, $\mu_s = 4\ \mu_0, \mu_s\mu_r = 2\ \mu_0, \mu_g\mu_s = 0.4\ \mu_0, \varepsilon_s\varepsilon_r = 2\varepsilon_0$ and $\varepsilon_g\varepsilon_s = 0.4\varepsilon_0$.

In Fig. 6, it is observed that the backscattering RCS at $\theta_k = 0^\circ$ is insensitive to the azimuthal angle ϕ_k varying from 0° to 360°. Interestingly, great variation of backscattering is pronounced as the incident angle increases gradually up to 90° and backscattering is fluctuating along the variation of the azimuthal angle. At $\theta_k = 90^\circ$, the backscattering reaches its maximum at $\phi_k = 0^\circ$ and 360°. At $\theta_k = 62^\circ$ and $\phi_k = 360^\circ$, backscattering reaches its minimum.

IV. Conclusion

The problem of electromagnetic scattering by a gyrotropic-coated conducting sphere has been successfully solved at a fixed laboratory frame for RCS observation. Hence, an incident wave from arbitrary illumination angles can be treated analytically. Two excellent agreements were observed, which verify the accuracy of our proposed approach and the correctness of the source code. The dependences of radar cross section on incident angle, radius ratio, and joint gyrotropic contrasts can be, for the first time, investigated in both lossless and lossy gyrotropic media. In addition, the significance of the incident and azimuthal angles in the RCS is illustrated, which has not been shown previously. On the other hand, if the incoming wave is kept unchanged, one can also rotate the gyrotropic object and the RCS along the backward direction can be manipulated. Our present analytical approach is expected to investigate a multi-layered gyrotropic sphere that has wide applications in antenna design, satellite communication and target shielding.

Appendix

The unknown coefficients in (6) are given as follows and in (A-2e and A-2f) at the top of the next page.

$$\mu_r' = \frac{\mu_r}{\mu_r^2-\mu_g^2}; \mu_g' = -\frac{\mu_g}{\mu_r^2-\mu_g^2}; \varepsilon_r' = \frac{\varepsilon_r}{\varepsilon_r^2-\varepsilon_g^2}; \varepsilon_g' = -\frac{\varepsilon_g}{\varepsilon_r^2-\varepsilon_g^2} \tag{A-1a}$$

$$\bar{\varepsilon}_r' = \varepsilon_r' - 1; \bar{\mu}_r' = \mu_r' - 1 \tag{A-1b}$$

$$\tilde{o}_{pq}^{mn} = \delta_{nq}\delta_{mp} + \left[\frac{(n^2+n-m^2)\bar{\varepsilon}_r' + m\varepsilon_g'}{n(n+1)}\right]\delta_{nq}\delta_{mp} \tag{A-2a}$$

$$\tilde{p}_{pq}^{mn} = \frac{i(n+m)[m\bar{\varepsilon}_r' - (n+1)\varepsilon_g']\delta_{n-1,q}\delta_{mp}}{n(2n+1)} + \frac{i(n-m+1)[m\bar{\varepsilon}_r' + n\varepsilon_g']\delta_{n+1,q}\delta_{mp}}{(n+1)(2n+1)} \tag{A-2b}$$

$$\tilde{q}_{pq}^{mn} = \frac{-i(n+m)\left[m\bar{\varepsilon}_r' - (n+1)\varepsilon_g'\right]\delta_{n-1,q}\delta_{mp}}{2n+1} + \frac{i(n-m+1)[m\bar{\varepsilon}_r' + n\varepsilon_g']\delta_{n+1,q}\delta_{mp}}{(2n+1)} \tag{A-2c}$$

$$\begin{aligned}\bar{p}_{pq}^{mn} &= \frac{[(2n^2+2n-3)m^2+(2n^2+2n-3)n(n+1)]\bar{\varepsilon}_r'+(4n^2+4n-3)m\varepsilon_g'}{n(n+1)(2n-1)(2n+3)}\delta_{nq}\delta_{mp} \\ &\quad + \delta_{nq}\delta_{mp} - \frac{(n+1)(n+m-1)(n+m)\bar{\varepsilon}_r'\delta_{n-2,q}\delta_{mp}}{(n-1)(2n-1)(2n+1)} - \frac{n(n-m+1)(n-m+2)\bar{\varepsilon}_r'\delta_{n+2,q}\delta_{mp}}{(n+2)(2n+1)(2n+3)} \end{aligned} \tag{A-2e}$$

$$\begin{aligned}\bar{q}_{pq}^{mn} &= -\frac{(n^2+n-3m^2)\bar{\varepsilon}_r'-m(2n-1)(2n+3)\varepsilon_g'}{(2n-1)(2n+3)}\delta_{nq}\delta_{mp} \\ &\quad + \frac{(n+1)(n+m-1)(n+m)\bar{\varepsilon}_r'\delta_{n-2,q}\delta_{mp}}{(2n-1)(2n+1)} - \frac{n(n-m+1)(n-m+2)\bar{\varepsilon}_r'\delta_{n+2,q}\delta_{mp}}{(2n+1)(2n+3)} \end{aligned} \tag{A-2f}$$

$$\begin{aligned}\bar{o}_{pq}^{mn} &= \frac{-i(n+m)(n+1)[m\bar{\varepsilon}_r'+(n-1)\varepsilon_g']\delta_{n-1,q}\delta_{mp}}{n(n-1)(2n+1)} \\ &\quad - \frac{i(n-m+1)n[m\bar{\varepsilon}_r'-(n+2)\varepsilon_g']\delta_{n+1,q}\delta_{mp}}{(n+1)(n+2)(2n+1)} \end{aligned} \tag{A-2d}$$

$\tilde{g}_{pq}^{uv}, \tilde{e}_{pq}^{uv}, \tilde{f}_{pq}^{uv}, \bar{g}_{pq}^{uv}, \bar{e}_{pq}^{uv}, \bar{f}_{pq}^{uv}$ can be obtained by changing $o, p, q, \bar{\varepsilon}_r'$, ϵ_g' and mn in (A-2) to $g, e, f, \bar{\mu}_r', \mu_g'$ and uv. The coefficients in (7) are shown as

$$\bar{d}_{pq} = \sum_{v,u}\frac{\bar{E}_{uv}}{\bar{E}_{pq}}\left(\tilde{g}_{pq}^{uv}d_{uv}+\bar{g}_{pq}^{uv}c_{uv}\right) \tag{A-3a}$$

$$\bar{c}_{pq} = \sum_{v,u}\frac{\bar{E}_{uv}}{\bar{E}_{pq}}\left(\tilde{e}_{pq}^{uv}d_{uv}+\bar{e}_{pq}^{uv}c_{uv}\right) \tag{A-3b}$$

$$\bar{w}_{pq} = \sum_{v,u}\frac{\bar{E}_{uv}}{\bar{E}_{pq}}\left(\tilde{f}_{mn}^{uv}d_{uv}+\bar{f}_{mn}^{uv}c_{uv}\right) \tag{A-3c}$$

$$\begin{aligned}\bar{w}_{00} &= \sum_{v,u}\frac{\bar{E}_{uv}}{\bar{E}_{pq}}\left(\tilde{f}_{00}^{uv}d_{uv}+\bar{f}_{00}^{uv}c_{uv}\right) \\ &= -\left[\left(\frac{2}{3}\right)^{\frac{1}{2}}\mu_g' d_{01}+\left(\frac{2}{15}\right)^{\frac{1}{2}}\bar{\mu}_t' c_{02}\right]E_0 \end{aligned} \tag{A-3d}$$

$$\bar{u}_{pq} = \sum_{v,u}\frac{\bar{E}_{uv}}{\bar{E}_{pq}}\left(\tilde{g}_{pq}^{uv}u_{uv}+\bar{g}_{pq}^{uv}v_{uv}\right) \tag{A-4a}$$

$$\bar{v}_{pq} = \sum_{v,u}\frac{\bar{E}_{uv}}{\bar{E}_{pq}}\left(\tilde{e}_{pq}^{uv}u_{uv}+\bar{e}_{pq}^{uv}v_{uv}\right) \tag{A-4b}$$

$$\bar{y}_{pq} = \sum_{v,u}\frac{\bar{E}_{uv}}{\bar{E}_{pq}}\left(\tilde{f}_{mn}^{uv}u_{uv}+\bar{f}_{mn}^{uv}v_{uv}\right) \tag{A-4c}$$

$$\begin{aligned}\bar{y}_{00} &= \sum_{v,u}\frac{\bar{E}_{uv}}{\bar{E}_{pq}}\left(\tilde{f}_{00}^{uv}u_{uv}+\bar{f}_{00}^{uv}v_{uv}\right) \\ &= -\left[\left(\frac{2}{3}\right)^{\frac{1}{2}}\mu_g' u_{01}+\left(\frac{2}{15}\right)^{\frac{1}{2}}\bar{\mu}_t' v_{02}\right]E_0 \end{aligned} \tag{A-4d}$$

The coefficients of the incident fields are given as follows

$$p_{mn} = [p_\theta\tilde{\tau}_{mn}(\cos\theta_k)-ip_\phi\tilde{\pi}_{mn}(\cos\theta_k)]e^{im\phi_k} \tag{A-5a}$$

$$q_{mn} = [p_\theta\tilde{\pi}_{mn}(\cos\theta_k)-ip_\phi\tilde{\tau}_{mn}(\cos\theta_k)]e^{im\phi_k} \tag{A-5b}$$

$$\tilde{\pi}_{mn}(\cos\theta) = C_{mn}\frac{m}{\sin\theta}P_n^m(\cos\theta) \tag{A-5c}$$

$$\tilde{\tau}_{mn}(\cos\theta) = C_{mn}\frac{d}{d\theta}P_n^m(\cos\theta) \tag{A-5d}$$

$$C_{mn} = \left[\frac{2n+1}{n(n+1)}\frac{(n-m)!}{(n+m)!}\right]^{\frac{1}{2}} \tag{A-6}$$

$$\sigma = \lim_{r\to\infty}4\pi\frac{d\sigma_{sca}}{d\Omega}, \quad \text{where } \frac{d\sigma_{sca}}{d\Omega} = |\mathrm{f}(\theta,\phi)|^2 \tag{A-7}$$

$$\mathbf{E_s} = E_o\mathrm{f}(\theta,\varphi)\frac{e^{ik_0r}}{r}, \quad r\to\infty \tag{A-8}$$

References

[1] J. A. Kong, *Electromagnetic Wave Theory*. Cambridge, MA, USA: EMW Publishing, 2005.

[2] G. Mie, "Beitrage zur Optik truber Medien speziell kolloidaler Metallosungen," *Ann. Phys.*, vol. 25, pp. 377–455, 1908.

[3] A. L. Aden and M. Kerker, "Scattering of electromagnetic wave from two concentric spheres," *J. Appl. Phys.*, vol. 22, pp. 1242–1246, 1951.

[4] J. D. Keener, K. J. Chalut, J. W. Pyhtila, and A. Wax, "Application of Mie theory to determine the structure of spheroidal scatters in biological materials," *Opt. Lett.*, vol. 32, no. 10, pp. 1326–1328, 2007.

[5] J. Dan, J. M. Jin, E. Michielssen, and D. J. Riley, "Time-domain finite-element simulation of three-dimensional scattering and radiation problems using perfectly matched layers," *IEEE Trans. Antennas Propag.*, vol. 51, no. 2, pp. 296–305, 2003.

[6] S. N. Papadakis, N. K. Uzunoglu, and C. N. Capsalis, "Scattering of a plane wave by a general anisotropic dielectric ellipsoid," *J. Opt. Soc. Am. A*, vol. 7, pp. 991–997, 1990.

[7] Y. L. Geng, X. B. Wu, L. W. Li, and B. R. Guan, "Mie scattering by a uniaxial anisotropic sphere," *Phys. Rev. E*, vol. 70, no. 5, p. 056609, 2004.

[8] C.-W. Qiu, S. Zouhdi, and A. Razek, "Modified spherical wave functions with anisotropy ratio: Application to the analysis of scattering by multilayered anisotropic shells," *IEEE Trans. Antennas Propag.*, vol. 55, no. 12, pp. 3515–3523, 2007.

[9] C. W. Qiu, L. W. Li, S. Zouhdi, T. S. Yeo, and Q. Wu, "On the integral identities consisting of two spherical Bessel functions," *IEEE Trans. Antennas Propag.*, vol. 55, no. 1, pp. 240–244, 2007.

[10] I. V. Lindell and A. H. Sihvola, "Transformation method for problems involving perfect electromagnetic conductor (PEMC) structures," *IEEE Trans. Antennas Propag.*, vol. 9, pp. 3005–3011, 2005.

[11] J. H. Richmond, "Scattering by a ferrite-coated conducting sphere," *IEEE Trans. Antennas Propag.*, vol. 35, no. 1, pp. 73–79, 1987.

[12] Y. Song and C. M. Tse, "EM scattering by a conducting sphere coated with a uniaxial layer under arbitrary illumination angle in a fixed laboratory frame," *Radioengineering*, vol. 20, no. 4, pp. 849–856, 2011.

[13] C. F. Bohren and D. R. Huffman, *Absorption and Scattering of Light by Small Particles*. New York, NY, USA: Wiley, 1983.

[14] Y. L. Geng and C. W. Qiu, Analytical spectral-domain scattering theory of a general gyrotropic sphere arXiv [Online]. Available: http://arxiv.org/abs/1102.4057, 2011

[15] X. Q. Sheng and Z. Peng, "Analysis of scattering by large objects with off-diagonally anisotropic material using finite element-boundary integral- multilevel fast multipole algorithm," *IET Microw. Antennas Propag.*, vol. 4, pp. 492–500, 2010.